Computer Physics Communications 135 (2001) 40–57

Computer Physics Communications

www.elsevier.nl/locate/cpc

Extension to the weighted histogram analysis method: combining umbrella sampling with free energy calculations

Marc Souaille [1], Benoît Roux *

Departments of Physics & Chemistry, Université de Montréal, C.P. 6128, succ. Centre-Ville, Canada H3C 3J7

Received 11 April 2000; accepted 27 April 2000

Abstract

The Weighted Histogram Analysis Method (WHAM) of Kumar et al. (J. Comput. Chem. 13 (1992) 1011), is used to combine free energy perturbations with umbrella sampling calculations. The formulation is general and allows optimal calculation of the free energies from a set of molecular dynamics simulations generated in the presence of arbitrary biasing umbrella sampling window potentials. The method yields the free energy associated with a given simulation as well as the probability distribution of the molecular system configurations by extracting the information contained in all the biased simulations (the windows) in an optimal way. The method presents some advantages compared to the standard free energy perturbation (FEP) and thermodynamic integration (TI) methods, because the window potential can be used for restricting the conformational space to specific regions during free energy calculations. © 2001 Published by Elsevier Science B.V.

Keywords: Simulations; Sampling; Biomolecules; Computer alchemy

1. Introduction

Computer simulations of detailed atomic models is a powerful approach for making progress in our understanding of the microscopic factors responsible for the conformational stability of biological macromolecules. An important class of computational problems require the calculation of the influence of amino acid substitutions on the relative thermodynamic stability of a protein in different conformational states. Such problems can be formulated, using an analysis based on thermodynamic cycles, in terms of the free energy difference corresponding to an alchemical transformation between two potential energy function, U_A and U_B [1,2]. Free energy perturbation (FEP) and thermodynamic integration (TI) represent the most widely employed techniques for calculating the alchemical free energy difference between U_A and U_B using computer simulations (see [1,2] for a review). As the

* Corresponding author. Current address: Department of Biochemistry and Structural Biology, Weill Medical College of Cornell University, 1300 York Avenue, New York, NY 10021, USA.

E-mail address: benoit_roux@med.cornell.edu (B. Roux).

[1] Current address: Phys. Chem. Inst., University of Zurich, Winterthurerstrasse 190, CH-8057 Zurich, Switzerland.

0010-4655/01/$ – see front matter
PII: S0010-4655(00)00215-0

free energy difference between two systems may be too large, it becomes computationally convenient to introduce a thermodynamic coupling parameter λ [3] for describing an unphysical intermediate system with potential energy $U(\lambda)$. The potential energy $U(\lambda)$ is constructed as a combination of those describing the true physical systems A and B such that their potential energy are recovered at the "end points", i.e. $U(\lambda = 0) = U_A$, and $U(\lambda = 1) = U_B$. The total free energy difference is then expressed as a sum of successive intermediate steps, in FEP, or as an integral over an average generalized force, in TI.

Different studies have shown that obtaining reliable results using the FEP or TI techniques is computationally expensive even for simple systems [9,10]. Although FEP and TI differ in their formulation, they are usually implemented in a very similar manner. A number of simulations corresponding to a set of discrete values $\{\lambda_i\}$ are first generated. The trajectories are then analyzed separately and the individual averages are combined together to yield the total free energy. Although formally correct, this procedure does not make full use of all accessible information that is present in the set of trajectories. For example, a trajectory generated with a particular value of the coupling parameter λ_i provides also some information about the distribution of the configurations corresponding to different values of the coupling parameter. Thus, the standard implementation of FEP or TI does not exploit the relationship between the set of trajectories and is thus not optimal. Furthermore, sampling problems may be encountered in FEP or TI when there are large energy barriers which prevent an effective exploration of the configurational space within the available computer time. In this case, well-converged averages are difficult to obtain directly from "straight" molecular dynamics trajectories. If the energy barrier can be associated to a particular generalized coordinate, such problem may be addressed by calculating explicitly the potential of mean force (PMF) [3] using special biased sampling techniques. One of these is the umbrella sampling technique of Torrie and Valleau [11]. In umbrella sampling, the microscopic system of interest is simulated in the presence of an artificial biasing window potential, W, introduced to enhance the sampling in the vicinity of a chosen region of configurational space (i.e. the biased simulations are generated using the biased potential energy $[U + W]$). The biasing potential W serves to confine the system around some region of configurational space, helping to achieve a more efficient sampling (this is the reason why the biasing potential W is called a "window" potential). A complete calculation requires a number of separate simulations, each biasing the configurational sampling around a different region of configurational space. Ultimately, the information from the various simulations must be unbiased and recombined together to obtain the final result.

A useful method for calculating free energies must thus enable one to extract all the available information provided by a set of simulations with different λ_i and biased sampling potentials W_j in an optimal way. The weighted histogram analysis method (WHAM) proposed by Kumar et al. [5] can be used to achieve this goal. WHAM represents a generalization and an extension of the histogram method developed by Ferrenberg and Swendsen [4]. It allows to obtain better estimates by combining the results of all the different simulations. The central idea, which goes back to the maximum overlap method developed by Bennet [6], consists in constructing an optimal estimate of the unbiased distribution function as a weighted sum over the data extracted from all the simulations and determining the functional form of the weight factors that minimizes the statistical error. WHAM is now routinely used to compute a PMF [5,7,13–18] or solvation free energy differences [5,8]. Nonetheless, the full strength of WHAM has not been exploited so far.

In this paper, we further explore some of the possibilities of WHAM for combining biasing potentials and free energy perturbations simultaneously. In particular, we show how WHAM can be used to compute averages of arbitrary quantities. We then show how additional biasing umbrella potentials can be introduced during free energy calculations. For the sake of completeness the derivation of the WHAM equations is reviewed briefly. The theoretical developments are illustrated with simple examples and a generic computer source code is given in Appendix.

2. Theoretical developments

2.1. The weighted histogram analysis method

In this section we briefly review the basis of WHAM. The goal is to get an optimal unbiased probability distribution $\rho_0(\eta)$, where η is some reaction coordinate, from a set of simulations performed with a perturbing potentials. Let us consider a reference molecular system with the potential energy $U_0(\mathbf{R})$, where $\mathbf{R}$ is the set of atomic coordinates. The reaction coordinate η is a function of the atomic coordinates, i.e. $\eta(\mathbf{R})$. Let us suppose that a set of molecular simulation has been performed using potential energy functions of the form,

$$U_0(\mathbf{R}) + W_i\big(\eta(\mathbf{R})\big), \tag{1}$$

where $W_i(\eta(\mathbf{R}))$ is some perturbing potential. From these simulations a set of biased probability distributions $\{\rho_i^{(b)}(\eta)\}$ can be obtained. $\rho_i^{(b)}(\eta)$ is computed as normalized histogram of the values of η occurring during the simulation i. The corresponding unbiased probability distribution $\rho_i^{(u)}(\eta)$ from simulation i is defined as,

$$\rho_i^{(u)}(\eta) = \mathrm{e}^{\beta[W_i(\eta)-f_i]}\rho_i^{(b)}(\eta), \tag{2}$$

where f_i is the free energy coming from the adding of the biasing potential $W_i(\eta(\mathbf{R}))$ to the reference potential $U_0(\mathbf{R})$. In the following, the free energies $\{f_i\}$ are assumed to be known, the method providing a posteriori an algorithm for their computation.

It has been shown that the WHAM method simplifies considerably the task of recombining together the unbiased histograms $\rho_i^{(u)}(\eta)$ to get the total probability distribution $\rho_0(\eta)$ [7]. It consists in writing $\rho_0(\eta)$ as a linear η-dependent combination of the unbiased probability distribution,

$$\rho_0(\eta) = C\sum_{i=1}^{N} p_i(\eta)\rho_i^{(u)}(\eta), \tag{3}$$

where C is a normalization constant. The weights are required to be normalized,

$$\sum_{i=1}^{N} p_i(\eta) = 1 \tag{4}$$

and they are chosen so as to minimize the statistical error made on the total probability distribution, that is, for any given value of η,

$$\frac{\partial(\sigma^2[\rho_0(\eta)])}{\partial p_i} = 0. \tag{5}$$

Then $\rho_0(\eta)$ takes the form,

$$\rho_0(\eta) = C\sum_{i=1}^{N} \frac{n_i \mathrm{e}^{-\beta[W_i(\eta)-f_i]}}{\sum_{j=1}^{N} n_j \mathrm{e}^{-\beta[W_j(\eta)-f_j]}}\rho_i^{(u)}(\eta) \tag{6}$$

$$= C\sum_{i=1}^{N} \frac{n_i}{\sum_{j=1}^{N} n_j \mathrm{e}^{-\beta[W_j(\eta)-f_j]}}\rho_i^{(b)}(\eta). \tag{7}$$

The derivation of Eq. (6) is given in the Appendix.

Until now, the treatment assumed that the free energy parameters $\{f_i\}$ were known. In fact, these parameters can be obtain self-consistently. Indeed, the definition of the free energy f_k is,

$$\mathrm{e}^{-\beta f_k} = \int \mathrm{d}\eta\, \rho_0(\eta)\mathrm{e}^{-\beta W_k(\eta)} \tag{8}$$

$$= C \int \mathrm{d}\eta \sum_{i=1}^{N} \frac{n_i \mathrm{e}^{-\beta W_k(\eta)}}{\sum_{j=1}^{N} n_j \mathrm{e}^{-\beta[W_j(\eta)-f_j]}} \rho_i^{(b)}(\eta). \tag{9}$$

The set of parameters $\{f_i\}$ appear on the left and on the right of Eq. (9) which can be solved iteratively. A first guess of values $\{f_i^0\}$ is used on the RHS of (9) to compute a new set of values $\{f_i^1\}$ which are in turn used as the new guess to compute $\{f_i^2\}$ and so on until convergence of the process. To get rid of the constant C, one may introduce an additional constraint on the free energy parameters or on the unbiased distribution function. For example, subtracting the offset constant f_0 from all the f_i is equivalent to assuming that the distribution $\rho_0(\eta)$ is normalized. In the following, the constant C will be omitted.

WHAM has been previously applied for the computation of a PMF [5,7,13–18] and free energies [5,8] by molecular dynamics simulation. In the following, we used the method to compute averages of arbitrary quantities.

2.2. Using WHAM for computing averages

In the previous section, the dependence of the coordinate η on the set of atomic coordinates $\mathbf{R}$ was not specified. The formulation is valid for any dimension of the coordinate η, and particularly in the case where $\eta \equiv \mathbf{R}$. Replacing η by $\mathbf{R}$, Eq. (7) becomes

$$\rho_0(\mathbf{R}) = \sum_{i=1}^{N} \frac{n_i}{\sum_{j=1}^{N} n_j \mathrm{e}^{-\beta[W_j(\mathbf{R})-f_j]}} \rho_i^{(b)}(\mathbf{R}). \tag{10}$$

In the previous expression, $\rho_0(\mathbf{R})$ is the optimal distribution of configurations $\mathbf{R}$ corresponding to the potential $U_0(\mathbf{R})$, obtained from the set of simulations using biased potential energy functions of the form $U_0(\mathbf{R}) + W_i(\mathbf{R})$, and $\rho_i^{(b)}(\mathbf{R})$ is the actual distribution of configurations occurring during the ith of these simulations. It may be formally expressed as,

$$\rho_i^{(b)}(\mathbf{R}) \equiv \frac{1}{n_i} \sum_{l=1}^{n_i} \delta(\mathbf{R} - \mathbf{R}_{i,l}), \tag{11}$$

where $\mathbf{R}_{i,l}$ is the lth of these configurations.

The free energies corresponding to the different biasing potentials can be computed using the distribution $\rho_0(\mathbf{R})$, thus,

$$\mathrm{e}^{-\beta f_k} = \int \mathrm{d}\mathbf{R}\, \mathrm{e}^{-\beta W_k(\mathbf{R})} \rho_0(\mathbf{R}) \tag{12}$$

$$= \int \mathrm{d}\mathbf{R} \sum_{i=1}^{N} \frac{n_i \mathrm{e}^{-\beta W_k(\mathbf{R})}}{\sum_{j=1}^{N} n_j \mathrm{e}^{-\beta[W_j(\mathbf{R})-f_j]}} \rho_i^{(b)}(\mathbf{R}) \tag{13}$$

$$= \int \mathrm{d}\mathbf{R} \sum_{i=1}^{N} \frac{\mathrm{e}^{-\beta W_k(\mathbf{R})}}{\sum_{j=1}^{N} n_j \mathrm{e}^{-\beta[W_j(\mathbf{R})-f_j]}} \sum_{l=1}^{n_i} \delta(\mathbf{R} - \mathbf{R}_{i,l}) \tag{14}$$

$$= \sum_{i=1}^{N} \sum_{l=1}^{n_i} \frac{\mathrm{e}^{-\beta W_k(\mathbf{R}_{i,l})}}{\sum_{j=1}^{N} n_j \mathrm{e}^{-\beta[W_j(\mathbf{R}_{i,l})-f_j]}}. \tag{15}$$

As in Eq. (9), the free energies are obtained self-consistently. However, the probability distributions $\rho_i^{(b)}(\mathbf{R})$ appear only as a formal quantities and do not need to be computed explicitly.

Instead of $\rho_0(\mathbf{R})$, the optimal biased probability distribution $\rho_k(\mathbf{R})$ corresponding to the kth perturbation potential $U_0(\mathbf{R}) + W_k(\mathbf{R})$ could be chosen. As as done for $\rho_0(\mathbf{R})$, the distribution $\rho_k(\mathbf{R})$ can be expressed as a linear combination of unbiased probability distributions

$$\rho_k(\mathbf{R}) = C' \sum_{i=1}^{N} p'_i(\mathbf{R}) \rho_i^{(u)}(\mathbf{R}), \tag{16}$$

where

$$\rho_i^{(u)}(\mathbf{R}) = \mathrm{e}^{\beta[W_i(\mathbf{R}) - W_k(\mathbf{R}) - f_i + f_k]} \rho_i^{(b)}(\mathbf{R}). \tag{17}$$

This time, the probability distributions $\rho_i^{(u)}(\mathbf{R})$ are not unbiased with respect to $U_0(\mathbf{R})$ but to $U_0(\mathbf{R}) + W_k(\mathbf{R})$. Instead of proceeding in this way, $\rho_k(\mathbf{R})$ can be directly obtained from $\rho_0(\mathbf{R})$ by using an analog of Eq. (2), that is,

$$\rho_k(\mathbf{R}) = \mathrm{e}^{-\beta[W_k(\mathbf{R}) - f_k]} \rho_0(\mathbf{R}). \tag{18}$$

Thus, once the free energies $\{f_i\}$ have been computed a set of optimal probability distributions $\rho_k(\mathbf{R})$ is formally available. The average of any quantity of interest can then be computed. For example, the average energy of the simulation k is,

$$\left\langle U_0(\mathbf{R}) + W_k(\mathbf{R}) \right\rangle_k = \int \mathrm{d}\mathbf{R} \left[U_0(\mathbf{R}) + W_k(\mathbf{R}) \right] \rho_k(\mathbf{R}) \tag{19}$$

$$= \sum_{i=1}^{N} \sum_{l=1}^{n_i} \frac{[U_0(\mathbf{R}_{i,l}) + W_k(\mathbf{R}_{i,l})] \mathrm{e}^{-\beta[W_k(\mathbf{R}_{i,l}) - f_k]}}{\sum_{j=1}^{N} n_j \mathrm{e}^{-\beta[W_j(\mathbf{R}_{i,l}) - f_j]}}. \tag{20}$$

The previous expressions are particularly simple to use in conjunction with a coupling parameter λ, describing the conversion from one molecular system to another. In this case the total potential energy function is,

$$U(\mathbf{R}, \lambda) = (1 - \lambda) U_0(\mathbf{R}) - \lambda U_1(\mathbf{R}) \tag{21}$$

$$= U_0(\mathbf{R}) + \lambda W(\mathbf{R}), \tag{22}$$

where

$$W(\mathbf{R}) = U_1(\mathbf{R}) - U_0(\mathbf{R}). \tag{23}$$

To compute the free energy difference between the two systems ($\lambda = 0$ and $\lambda = 1$), a set of simulations is performed corresponding to a predefined set of values of λ. The simulation i is performed using the potential energy function $U_0(\mathbf{R}) + W_i(\mathbf{R})$ where $W_i(\mathbf{R}) \equiv \lambda_i W(\mathbf{R})$.

2.3. Umbrella sampling combined with free energy perturbation

The calculation of the free energy associated with a transformation with a coupling parameter often requires an extensive conformational sampling for particular degrees of freedom. In principle, umbrella sampling is the method of choice to enhance the exploration of the conformational space in a given region. It is thus of interest to combine biased sampling methods with those of free energy simulations within the framework of WHAM. In this case, the perturbing potential can be written as the sum of two terms,

$$W_{ij}(\mathbf{R}) = \lambda_i W_0(\mathbf{R}) + K_j \left(\eta'(\mathbf{R}) - \eta_j \right)^2, \tag{24}$$

where

$$W_0(\mathbf{R}) = U_1(\mathbf{R}) - U_0(\mathbf{R}). \tag{25}$$

The first term corresponds to the transformation from one molecular system to the other, and the second term is an umbrella sampling potential. WHAM allows the calculation of the free energy corresponding to the biasing

potential $\lambda W_0(\mathbf{R})$ using the information contained in the whole set of trajectories in an optimal manner. Moreover, it can be used to calculate the PMF along the coordinate η, as a function of λ.

The procedure is the following. Once the set of trajectories has been computed, the first step is to calculate the free energies associated with each biasing potential $W_{ij}(\mathbf{R})$. This is acomplished exactly in the same manner as previously, using an iterative procedure, i.e.

$$\mathrm{e}^{-\beta f_{mn}} = \int \mathrm{d}\mathbf{R}\, \mathrm{e}^{-\beta W_{mn}(\mathbf{R})} \rho_0(\mathbf{R}) \tag{26}$$

$$= \int \mathrm{d}\mathbf{R} \sum_{i,j=1}^{N} \frac{n_{ij}\, \mathrm{e}^{-\beta W_{mn}(\mathbf{R})}}{\sum_{k,l=1}^{N} n_{kl}\, \mathrm{e}^{-\beta[W_{kl}(\mathbf{R})-f_{kl}]}} \rho_{ij}^{(b)}(\mathbf{R}) \tag{27}$$

$$= \sum_{i,j=1}^{N} \sum_{p=1}^{n_{ij}} \frac{\mathrm{e}^{-\beta W_{mn}(\mathbf{R}_{ij,p})}}{\sum_{k,l=1}^{N} n_{kl}\, \mathrm{e}^{-\beta[W_{kl}(\mathbf{R}_{ij,p})-f_{kl}]}}, \tag{28}$$

where f_{ij} is free energy associated with the biasing potential $W_{ij}(\mathbf{R})$, and $\mathbf{R}_{ij,p}$ is the pth configuration of the corresponding trajectory.

As mentioned above, the optimal probability distribution $\rho_0(\mathbf{R})$ is formally available once the free energies associated with each window are computed. From this distribution, the desired free energy $F(\lambda)$ can be computed,

$$\mathrm{e}^{-\beta F(\lambda)} \equiv \int \mathrm{d}\mathbf{R}\, \mathrm{e}^{-\beta\lambda W_0(\mathbf{R})} \rho_0(\mathbf{R}) \tag{29}$$

$$= \int \mathrm{d}\mathbf{R} \sum_{i,j=1}^{N} \frac{n_{ij}\, \mathrm{e}^{-\beta\lambda W_0(\mathbf{R})}}{\sum_{k,l=1}^{N} n_{kl}\, \mathrm{e}^{-\beta[W_{kl}(\mathbf{R})-f_{kl}]}} \rho_{ij}^{(b)}(\mathbf{R}) \tag{30}$$

$$= \sum_{i,j=1}^{N} \sum_{p=1}^{n_{ij}} \frac{\mathrm{e}^{-\beta\lambda W_0(\mathbf{R}_{ij,p})}}{\sum_{k,l=1}^{N} n_{kl}\, \mathrm{e}^{-\beta[W_{kl}(\mathbf{R}_{ij,p})-f_{kl}]}}. \tag{31}$$

To obtain the PMF corresponding to a particular value of λ, the corresponding optimal probability distribution,

$$\rho(\mathbf{R},\lambda) = \rho_0(\mathbf{R})\mathrm{e}^{-\beta[\lambda W_0(\mathbf{R})-F(\lambda)]} \tag{32}$$

is first needed. Then, the desired normalized histogram is computed,

$$\rho(\eta,\lambda) = \int \mathrm{d}\mathbf{R}\, \rho(\mathbf{R},\lambda)\, \delta\big(\eta - \eta'(\mathbf{R})\big) \tag{33}$$

$$= \sum_{i,j=1}^{N} \sum_{p=1}^{n_{ij}} \frac{\mathrm{e}^{-\beta[\lambda W_0(\mathbf{R}_{ij,p})-F(\lambda)]}}{\sum_{k,l=1}^{N} n_{kl}\, \mathrm{e}^{-\beta[W_{kl}(\mathbf{R}_{ij,p})-f_{kl}]}}\, \delta\big(\eta - \eta'(\mathbf{R}_{ij,p})\big). \tag{34}$$

Finally, the λ-dependent PMF is,

$$w(\eta,\lambda) = -k_B T \log\big[\rho(\eta,\lambda)\big]. \tag{35}$$

3. Computational illustrations

3.1. Charge–dipole interaction

As a first illustration of the method, we consider a simple system consisting of a point charge and a dipole separated by a fixed distance. The advantage of this simple model is that there exists a simple relation between the

average and the free energy of the system in the high temperature approximation, providing a very simple test of the validity of Eq. (20).

The interaction energy U for this charge–dipole system is,

$$U = -\vec{\mu}.\vec{E}, \tag{36}$$

where $\vec{\mu}$ is the point dipole and $\vec{E}$ is the value at the dipole location of the electric field created by the point charge. The excess free energy in respect to an infinite separation is,

$$F = -\frac{1}{\beta}\log\left\{\int \mathrm{d}\omega\, \mathrm{e}^{\beta\vec{\mu}.\vec{E}}\right\}, \tag{37}$$

where $\beta = 1/k_B T$ and ω represents the degrees of freedom of the problem, that is the polar angles θ and ϕ characterizing the orientation in space of the dipole. In the high-temperature limit, the interaction energy is much lower than the thermal energy, i.e.

$$\vec{\mu}.\vec{E} \ll k_B T. \tag{38}$$

Expanding the integral of Eq. (37) to the second order in the quantity $\beta(\vec{\mu}.\vec{E})$, it can be easily shown that

$$F = -\frac{1}{\beta}\log\left(1 + \frac{1}{6}\beta^2\mu^2E^2\right) \tag{39}$$

$$\simeq -\frac{1}{6}\beta\mu^2E^2. \tag{40}$$

To calculate the mean energy, its expression in terms of the free energy derivative is used,

$$\langle U\rangle = \frac{\partial(\beta F)}{\partial\beta} \tag{41}$$

which gives,

$$\langle U\rangle = -\frac{2}{6}\beta\mu^2E^2 \tag{42}$$

$$= 2F. \tag{43}$$

It can be seen in the preceding expression that the average energy is just twice the free energy in the high-temperature limit.

To sample the configuration of this point charge-point dipole system, we performed a Langevin molecular dynamics on a system consisting of a point ion and a water molecule. The position of the ion and of the oxygen atom were maintained fixed. The distance separation was 15 Å. Ten windows were used to increase the charge of the ion by a factor λ from 0.05e to 0.95e by increments of 0.1e. Each window consisted in 5 ps of equilibration, followed by 10 ps of production during which the values $U_0(\mathbf{R})$ and $W(\mathbf{R})$ were stored. The time step was 0.001 ps and a friction constant of 25 ps^{-1} was applied on the hydrogen atoms. To compare the results with a more standard technique, the same simulation was used to perform thermodynamics perturbation calculation.

The results are shown on Fig. 1. As expected, the free energy is a quadratic function of λ since the electric field is proportional to the charge of the ion. The free energy F_{WHAM} obtained from the WHAM algorithm compares well to F_{FEP} obtained from the free energy perturbation technique (FEP), especially at $\lambda = 1$ where both approaches give nearly the same value. Nonetheless, F_{WHAM} is slightly smoother than F_{FEP} because the fluctuations are distributed over all the windows in this case.

We have also computed the average energy for each windows, first using Eq. (20), this quantity is denoted $\langle U\rangle_{\mathrm{WHAM}}$ and second by averaging the data corresponding to the potential energy $U_{\lambda_i}(\mathbf{R})$ of the window λ_i only. This quantity is denoted $\langle U\rangle_\lambda$. It turns out that $\langle U\rangle_{\mathrm{WHAM}}$ is a nearly perfect parabola, related to F_{WHAM} by a factor 2, whereas $\langle U\rangle_\lambda$ follows only roughly this trend with large fluctuations.

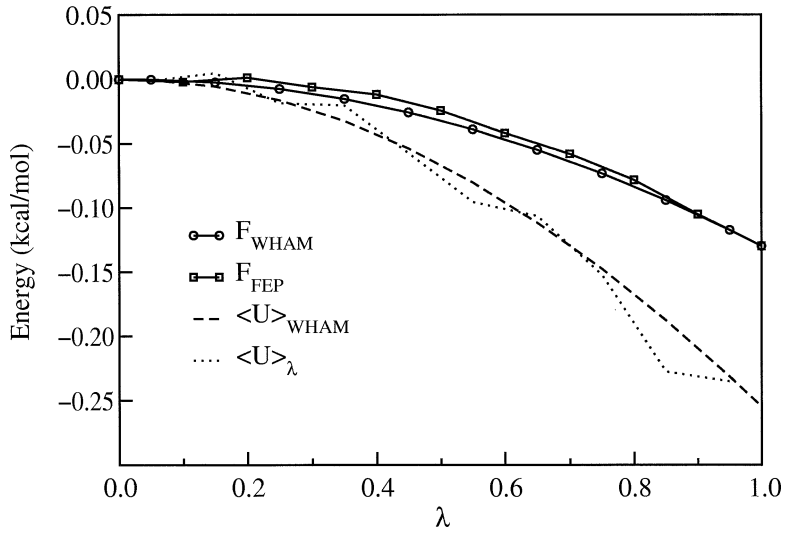

Fig. 1. Free energy and average energy as a function of the coupling parameter, for a charge–dipole system.

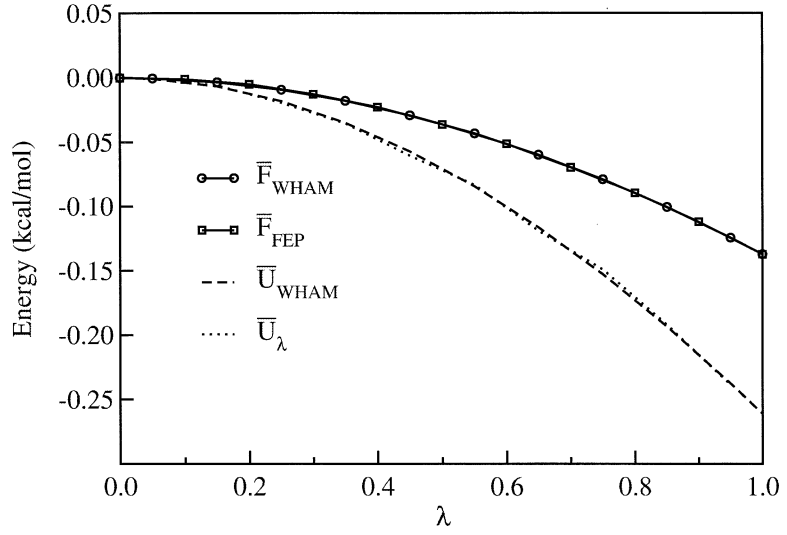

Fig. 2. Free energy and average energy as a function of the coupling parameter, for a charge–dipole system. Each curve is averaged over a set of 100 simulations.

To make a deeper comparison between the methods, we generated a series a 100 simulations with the same conditions as described previously. From the data of each simulation, we have computed F_{WHAM}, F_{FEP}, $\langle U\rangle_{\mathrm{WHAM}}$ and $\langle U\rangle_{\lambda}$. These quantities have been averaged over the set of simulation, leading to $\overline{F}_{\mathrm{WHAM}}$, $\overline{F}_{\mathrm{FEP}}$, $\overline{U}_{\mathrm{WHAM}}$ and $\overline{U}_{\lambda}$, respectively. They are shown in Fig. 2. The corresponding root mean square deviation δF_{WHAM}, δF_{FEP}, δU_{WHAM} and δU_{λ} where also computed. They are shown in Fig. 3. Averaging over the set of simulations (Fig. 2) gives the same result for the free energies F_{WHAM} and F_{FEP}, and for the average energies $\langle U\rangle_{\mathrm{WHAM}}$ and $\langle U\rangle_{\lambda}$. As shown in Fig. 3, the free energy calculated from WHAM and FEP have similar standard deviations in the case of the free energy. However, the statistical error made on the average

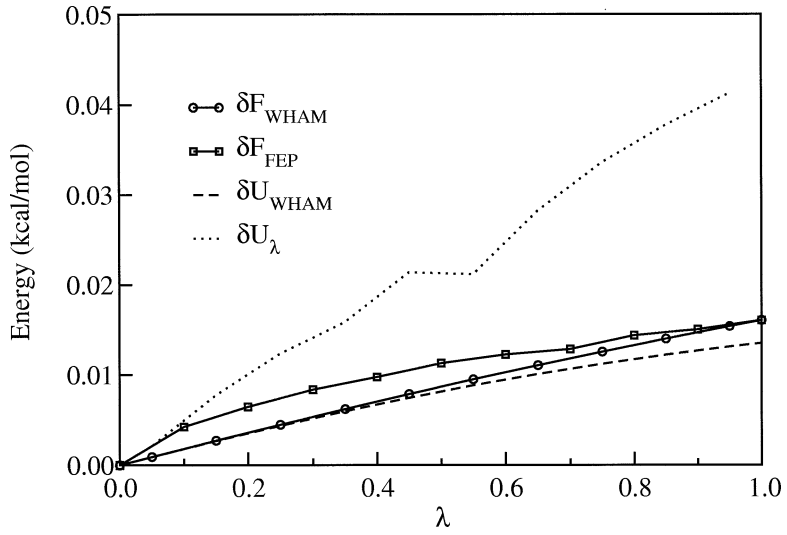

Fig. 3. Mean square deviation of the free energy and the average energy as a function of the coupling parameter, for a charge–dipole system, from a set of 100 simulations (see text).

energy depends strongly on the computational approach. The average energy calculated from WHAM using Eq. (20) reduces considerably the statistical error relative to a simple window-based averaging. The standard deviation of the average energy is similar in magnitude to that of the free energy with WHAM. In contrast, the standard deviation of a simple window-based averaging averaging is much larger than that of the free energy.

3.2. Solvation energies

We used Eq. (15) to calculate the solvation free energy (excess chemical potential) of small solutes in water, i.e. a potassium ion K^+, a water molecule and an argon atom. The solute was inserted in a sphere of explicit solvent water molecules using $N = 22$ windows. The water molecules were modeled on the basis of the TIP3 potential [21] and a spherical solvent boundary potential (SSBP) [20] was used to simulate the infinite solvent bulk. For each solute, three simulations were performed, with 25, 50 and 100 explicit solvent molecules. A harmonic constraint of 1 kcal/mol/Å^2 was applied to keep the center of mass of the solute at the center of the sphere. Each window consisted in 2 ps of equilibration followed by 8 ps of production during which the values $U_0(\mathbf{R})$ and $W(\mathbf{R})$ were stored. All simulations were performed with Langevin dynamics using the program CHARMM [19]. The time step was 0.001 ps and a friction constant of 5 ps^{-1} was applied on all the oxygen atoms. We chose the values of λ such as, $\lambda_k = (k/(N-1))^5$, for $k = 0 \ldots N-1$. Eq. (15) was iterated until the changes in the free energies $\{f_i\}$ was less than 0.001. As a check, the free energy differences from the same simulations was calculated using FEP. Moreover the average energy difference $\langle U_1 \rangle_1 - \langle U_0 \rangle_0$ was calculated using Eq. (20). This quantity is denoted $\langle \Delta U \rangle_W$. The results for various numbers of explicit water molecules are given in Table 1. For each solute, the solvation free energies are very similar whatever the number of solvent molecules. Moreover, the agreement between the two methods employed indicates that the WHAM algorithm is at least as good as FEP for this kind of calculation.

Table 1
Solvation free energies (excess chemical potential) and average energies for three different solute in 25, 50 and 100 explicit water molecules. A SSBP potential [20] has been added to simulate the infinite bulk. The column labeled FEP correspond to the free energy calculated using free energy perturbation. The column labeled WHAM corresponds to the solvation free energy calculation using Eq. (15). The column $\langle \Delta U \rangle_W$ corresponds to the average energy difference $\langle U_1 \rangle_1 - \langle U_0 \rangle_0$ calculated using Eq. (20)

	25 mol.			50 mol.			100 mol.		
Solute	FEP	WHAM	$\langle \Delta U \rangle_W$	FEP	WHAM	$\langle \Delta U \rangle_W$	FEP	WHAM	$\langle \Delta U \rangle_W$
K^+	−79.57	−78.96	−83.97	−81.36	−80.69	−77.76	−80.74	−80.11	−79.50
H_2O	−5.41	−5.43	−7.96	−5.38	−5.31	−6.04	−5.92	−5.88	−10.44
Ar	3.66	3.89	−0.11	3.75	3.79	9.04	3.38	3.39	−5.93

Table 2
The same as Table 1 except that 100 ps of data were used per window instead of 10 ps

	25 mol.		50 mol.		100 mol.	
Solute	WHAM	$\langle \Delta U \rangle_W$	WHAM	$\langle \Delta U \rangle_W$	WHAM	$\langle \Delta U \rangle_W$
K^+	−78.47	−78.33	−79.66	−85.63	−80.60	−87.16
H_2O	−5.12	−9.97	−5.14	−5.94	−5.65	−11.13
Ar	3.71	0.88	3.94	2.60	3.30	1.41

3.3. Charge–charge interaction

As an illustration of the combined umbrella sampling-free energy perturbation, we first consider the interaction between one fixed charge equal to λq_1 and a moving particle with a charge q_2. The potential energy function of this system is,

$$U(\mathbf{R}, \lambda) = \lambda W_0(\mathbf{r}_1, \mathbf{r}_2) = \lambda \frac{q_1 q_2}{r}, \tag{44}$$

where $r = |\mathbf{r}_1 - \mathbf{r}_2|$ is the distance separation between the particles. Due to the spherical symmetry of the system, this quantity appears as the natural reaction coordinate, i.e. $\eta = r$. If r is restrained between two boundary values r_a and r_b, the free energy is

$$F(\lambda) = -\frac{1}{\beta} \log \left\{ \frac{\int_{r_a}^{r_b} 4\pi r^2 \mathrm{e}^{-\beta \lambda q_1 q_2 / r} \, \mathrm{d}r}{\int_{r_a}^{r_b} 4\pi r^2 \, \mathrm{d}r} \right\}. \tag{45}$$

The previous free energy was calculated according to Eq. (45) from a set of molecular dynamic simulations using its integral expression and the trapezoidal rule. The value of r_a and r_b were 5 and 10 Å, respectively. For each simulation an umbrella potential was used to restrain the distance between the two particles. The potential energy function used for the simulation (i, j) was,

$$W_{ij}(\mathbf{r}_1, \mathbf{r}_2) = \lambda_i \frac{q_1 q_2}{r} + K(r - r_j)^2. \tag{46}$$

All simulation were performed at 300 K with Langevin dynamics. K was set to 10 kcal/mol/Å^2 and $-q_1 = q_2 =$ 0.5e. The values of λ considered in the simulations were 0.0, 0.2, 0.4, 0.6 and 0.8. For each value of λ, r_j was varied from 5 to 10 Å with an 0.5 Å increment. The integration timestep was 1 fs, the length of each simulation was 200 ps and the data (the potential W_0 and the distance r) were recorded every 20 fs. 300 points were used for the trapezoidal rule.

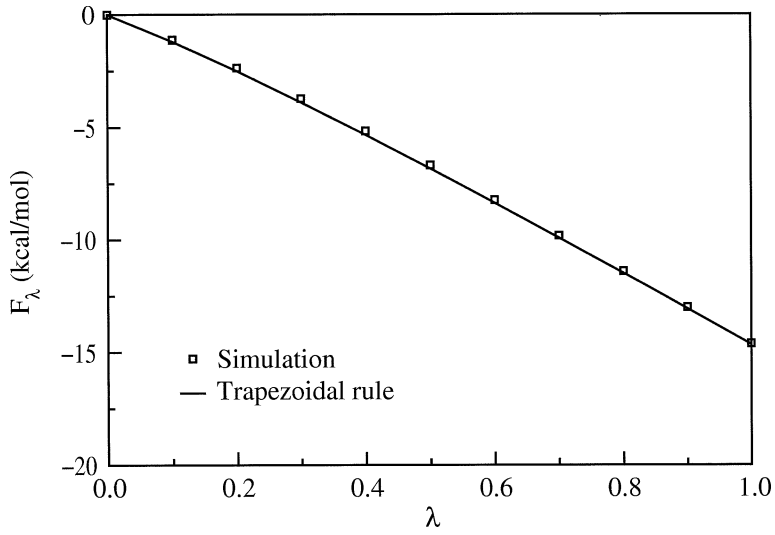

Fig. 4. Free energy as a function of the coupling parameter λ alone. The umbrella potential contribution has been integrated out using Eq. (31).

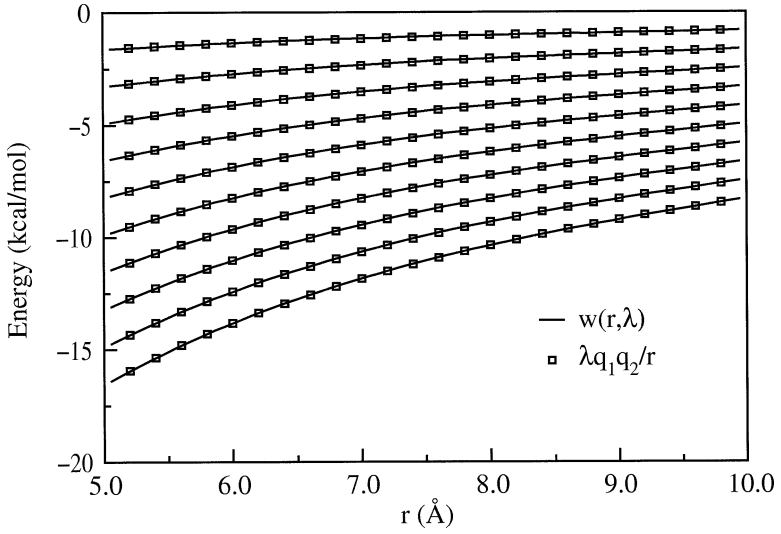

Fig. 5. Interaction energy between two charges calculated as a PMF, using Eqs. (34) and (35). From top to bottom, the values of λ go from 0.1 to 1.0 with a 0.1 increment. For comparison, the exact potential has been plotted.

Fig. 4 shows the free energy $F(\lambda)$ calculated by the two methods. The agreement is very good. As the figure shows, some values of λ that were not considered in the simulations were used a posteriori to calculate $F(\lambda)$. This interesting interpolation feature of WHAM has been mentioned previously concerning the calculation of a PMF [14]. Once the free energy $F(\lambda)$ has been computed for some particular values of λ, the corresponding probability distribution (30) is formally available. This is particularly useful when derivatives with respect to λ are necessary. From this distribution, we have calculated the PMF $w(r, \lambda)$, using Eq. (34). It is shown in Fig. 5. For the values of λ considered in the simulations, the different PMF $w(r, \lambda)$ could be obtained independently from each other using Eq. (7). The resulting curves (not shown) contain more statistical noise than those of Fig. 5. This

comes from the fact that in the second case, a PMF corresponding to a particular value of λ is calculated using the information contained in times series calculated with other values of λ. Moreover, as mentioned previously, Eq. (34) allows the computation of PMF corresponding to some values of λ not considered in the simulations.

3.4. Alchemical transformation of butane to glycol

As a last example, we consider the mutation from butane to glycol in vacuum and in explicit solvent, using in addition an umbrella potential to restrain the dihedral angle ϕ implying the four heavy atoms of the solute (the four carbon atoms in the case of butane and the two carbon atoms and the two oxygen atoms in the case of glycol) around some predefined values. Each CH_3 group was transformed into a OH group (single topology) using a coupling parameter λ. A set of simulation was performed using biasing potentials of the form,

$$W_{ij}(\mathbf{R}) = \lambda_i W_0(\mathbf{R}) + K_j\big(\phi(\mathbf{R}) - \phi_j\big)^2, \tag{47}$$

where

$$W_0(\mathbf{R}) = U_1(\mathbf{R}) - U_0(\mathbf{R}). \tag{48}$$

U_1 is the potential energy function of glycol and U_0 is the potential energy function of butane.

All simulations were performed with Langevin dynamics at 300 K using the program CHARMM [19]. For the simulations using explicit solvent, the solutes were immersed in 50 TIP3 water molecules [21] and a SSBP potential was applied to simulate the infinite bulk [20]. For all simulations (in vacuum or in solvent), seven reference ϕ_j values of the dihedral angle were considered in the umbrella potential, i.e. 0, 30, 60, 90, 120, 150 and 180 degrees and ten values of the coupling parameter were considered, calculated as,

$$\lambda_k = \frac{1}{2}\left\{1 + \tanh\left[\frac{2}{3}(k - N_w/2)\right]\right\}, \quad k = 2, \ldots, 9, \tag{49}$$

with $\lambda_1 = 0$ and $\lambda_{10} = 1$. Thus, a total of 70 different biasing potentials was thus considered. All force constants K_j were set to 8 kcal/mol/rad^2. Seven preliminary 20 ps simulations were performed with $\lambda = 0$, each one corresponding to a different reference value ϕ_j, in order to relax the harmonic constraint. Then a series of seven simulations was performed. In each simulation, the umbrella potential was maintained fixed, and the coupling parameter λ was increased every 55 ps, according to Eq. (49). For each of these 55 ps periods, data were collected during the last 50 ps, every 10 fs (5000 data points). Additional simulations corresponding to $\phi_j = 0$ and 120 degrees were performed for every value of λ during 50 ps (5000 data points).

Eq. (31) was used to computed the solvation free energy difference between the butane and glycol. The results are shown of Fig. 6. For this calculation, the values of λ were not the same as those considered during the simulations (see figure). The calculated total solvation free energy difference,

$$\Delta\Delta F_{\text{solv}} = (F_{1,s} - F_{1,v}) - (F_{0,s} - F_{0,v}) \tag{50}$$

$$= (F_{1,s} - F_{0,s}) - (F_{1,v} - F_{0,v}) \tag{51}$$

is equal to -10.0 kcal/mol, where the subscript $0, 1, s, v$ correspond to butane, glycol, solvent and vacuum, respectively.

Eqs. (34) and (35) were used to compute the PMF of butane and glycol ($\lambda = 0$ and 1, respectively) as a function of the dihedral angle. The results are shown on Fig. 7. The PMF of butane is essentially the same in vacuum or in water as expected for a non polar molecule. On the contrary the PMF of glycol presents lower barriers in solvent than in vacuum. The barriers occur for values of the dihedral angle corresponding to conformations where water molecule can establish hydrogen bonds connecting the two OH groups together, lowering the energy in respect to the vacuum case.

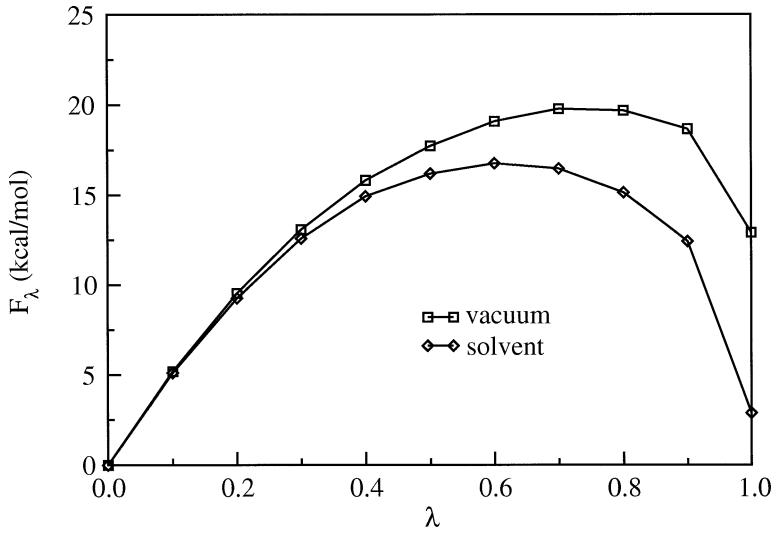

Fig. 6. Free energy as a function of the coupling parameter λ alone. The umbrella potential contribution has been integrated out using Eq. (31).

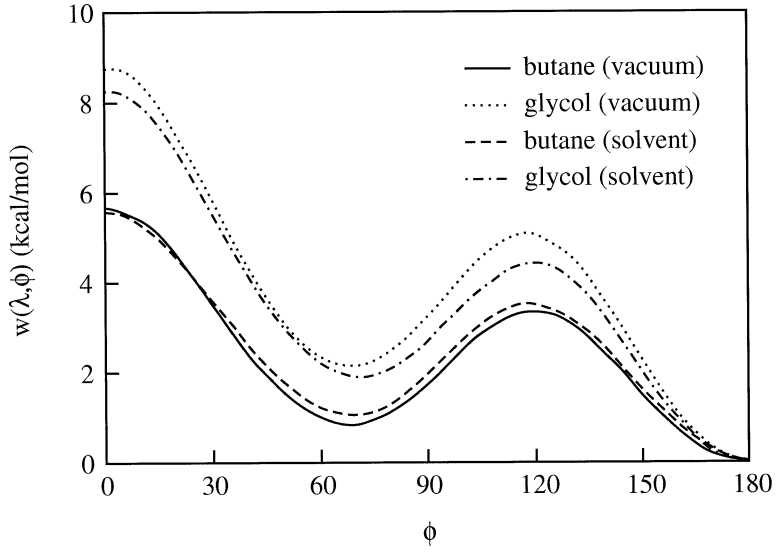

Fig. 7. PMF calculated using Eqs. (34) and (35).

4. Summary

WHAM allows the calculation, in a self-consistent way, of the free energies associated with arbitrary perturbations added to a reference potential [4,5]. In previous applications, the method has proven useful for calculating PMF's as function of a few coordinate (usually one or two) with the umbrella sampling technique [5,7,13–18]. In biomolecular simulations, it is also of interest to be able to calculate the free energies associated with alchemical transformation [1]. Such transformations of the potential energy function of the biomolecular system are usually mapped out using a coupling parameter called λ. This is the scheme normally used within

the framework of the TI or FEP techniques [1,2]. WHAM also allows the calculation of such alchemical transformation [5]. For example, it was used to obtain the electrostatic contribution to the solvation free energy for charging amino acids in liquid water [8].

In the current application, the free energy associated with both umbrella sampling window potentials as well as variations of a coupling parameter λ in the potential energy of the molecular system are combined into WHAM, in a unified fashion, for analysis of free energy differences. Most of the mathematical expressions are easily obtained, in relation with previous applications of WHAM, by considering the whole set of atomic coordinate **R** as a reaction coordinate. The corresponding multi-dimensional "histograms" resulting from the different biased simulations, which do not need to be computed explicitly, are then treated as formal quantities. A bias arising from the introduction of a coupling parameter or an umbrella sampling potential presents no essential difference. They are just biasing potentials. This allow to mix both kind of perturbations, when for example, one needs to better sample along some particular degrees of freedom during an alchemical transformation.

Such an application of WHAM presents some additional advantages relative to the traditional TI or FEP techniques. In particular, the free energy corresponding to a particular λ_i is computed using the information contained in the times series of all the simulations windows in an optimal way, a feature allowed by the formulation of WHAM. Moreover, we have shown that once the free energies of the different windows are computed, a set of optimal configuration distribution functions is available. Each element of the set corresponds to a biased potential added to the reference potential (i.e. to a given window λ_i). The average of arbitrary quantities may be computed using these distribution functions. In addition, the analysis provides the PMF along a given coordinate as a function of the coupling parameter.

Acknowledgements

This work was supported by grants from the Medical Research Council of Canada (MRC). B.R. is a research fellow of the MRC.

Appendix A. Derivation of the WHAM expressions

The minimization (5) under constraints is performed using the standard method of Lagrange multipliers. Assuming that all the simulations are statistically independent, the statistical error to be minimized is

$$\sigma^2\big[\rho_0(\eta)\big] = C\sum_{i=1}^{N} p_i^2(\eta)\sigma^2\big[\rho_i^{(u)}(\eta)\big] - \mu\left(\sum_{i=1}^{N} p_i(\eta) - 1\right), \tag{52}$$

where μ is the Lagrange multiplier. The weights satisfying Eq. (5) are,

$$p_i(\eta) = \frac{(\sigma^2[\rho_i^{(u)}(\eta)])^{-1}}{\sum_{j=1}^{N}(\sigma^2[\rho_j^{(u)}(\eta)])^{-1}} \tag{53}$$

and can be expressed in terms of $\sigma^2[\rho_i^{(b)}(\eta)]$ according to the relation,

$$\sigma^2\big[\rho_i^{(u)}(\eta)\big] = \mathrm{e}^{2\beta[W_i(\eta)-f_i]}\sigma^2\big[\rho_i^{(b)}(\eta)\big]. \tag{54}$$

The statistical error $\sigma^2[\rho_i^{(b)}(\eta)]$ of the computed histogram $\rho_i^{(b)}(\eta)$ may be expressed in the following form [12],

$$\sigma^2\big[\rho_i^{(b)}(\eta)\big] = \frac{g_i(\eta)}{n_i\Delta\eta}\overline{\rho_i^{(b)}(\eta)}, \tag{55}$$

where $\overline{\rho_i^{(b)}(\eta)}$ is the histogram computed from an infinite length simulation, n_i is the "length" of the simulation i, i.e. the number of coordinate sets used to compute $\rho_i^{(b)}(\eta)$. $\Delta\eta$ is the resolution of $\rho_i^{(b)}(\eta)$, that is the width of the bins used to calculate the histogram. Moreover,

$$g_i(\eta) = \left(1 + \frac{\tau_i(\eta)}{\delta t}\right), \tag{56}$$

where $\tau_i(\eta)$ is a correlation time and δt is the time step between two consecutive coordinate sets. The proof of (55) and the significance of $\tau_i(\eta)$ are given in the next section. We make the assumption that the factors $g_i(\eta)$ are the same for all the windows [5]. An estimate of $\overline{\rho_i^{(b)}(\eta)}$ is given by Eq. (2) where $\rho_i^{(b)}(\eta)$ is replaced by $\overline{\rho_i^{(b)}(\eta)}$ and $\rho_i^{(u)}(\eta)$ by the probability distribution we are looking for, i.e. $\rho_0(\eta)$.

$$\overline{\rho_i^{(b)}(\eta)} = \mathrm{e}^{-\beta[W_i(\eta)-f_i]}\rho_0(\eta). \tag{57}$$

Finally, using Eqs. (2), (53), (55) and (57), it can be easily shown that

$$p_i(\eta) = \frac{n_i \mathrm{e}^{-\beta[W_i(\eta)-f_i]}}{\sum_{j=1}^{N} n_j \mathrm{e}^{-\beta[W_j(\eta)-f_j]}}. \tag{58}$$

Another derivation of the last expression using Baysian probabilities can be found in Ref. [15].

Appendix B. Expression of the statistical error

Let us consider $\rho(\eta)$ the normalized probability distribution of a reaction coordinate η, computed from a molecular dynamics simulation. We will now show that the statistical error $\sigma^2[\rho(\eta)]$ made on this distribution has the following form,

$$\sigma^2\big[\rho(\eta)\big] = \frac{1}{n\Delta\eta}\left(1 + 2\frac{\tau(\eta)}{\delta t}\right)\overline{\rho(\eta)}, \tag{59}$$

where n is the number of consecutive set of coordinates used to compute $\rho(\eta)$, δt is the time interval between two such sets, τ is a correlation time and $\Delta\eta$ is the resolution of $\rho(\eta)$.

For this, let us consider the time series $\{\eta_k\}$ of values that takes the reaction coordinate during the simulation. $\rho(\eta)$ is computed as a normalized histogram, i.e. it is a sum of counters C_η,

$$\rho(\eta)\,\Delta\eta = \frac{1}{n}\sum_{k=1}^{n} C_\eta(\eta_k), \tag{60}$$

where C_η is defined as,

$$C_\eta(\eta_k) = \begin{cases} 1 & \text{if } \eta_k \in [\eta, \eta + \Delta\eta], \\ 0 & \text{otherwise.} \end{cases} \tag{61}$$

The statistical error is,

$$\sigma^2\big[\rho(\eta)\big] = \big\langle\big[\rho(\eta) - \overline{\rho(\eta)}\big]^2\big\rangle \tag{62}$$

$$= \frac{1}{\Delta\eta^2}\left\langle\left[\frac{1}{n}\sum_{k=1}^{n} C_\eta(\eta_k) - \langle C_\eta\rangle\right]^2\right\rangle \tag{63}$$

$$= \frac{1}{n\Delta\eta^2}\left(1 + 2\frac{\tau(\eta)}{\delta t}\right)\big(\langle C_\eta^2\rangle - \langle C_\eta\rangle^2\big), \tag{64}$$

where $\tau(\eta)$ is the correlation time given by,

$$\tau(\eta) = \sum_{k=1}^{n-1}\left(1-\frac{k}{n}\right)\frac{\langle \Delta C_\eta(\eta_0)\Delta C_\eta(\eta_k)\rangle}{\langle \Delta C_\eta\rangle^2} \tag{65}$$

$$\simeq \int_0^T \mathrm{d}t\left(1-\frac{t}{T}\right)\frac{\langle \Delta C_\eta(0)\Delta C_\eta(t)\rangle}{\langle \Delta C_\eta\rangle^2}, \tag{66}$$

where $T = n\,\delta t$ and $\Delta C_\eta = C_\eta - \langle C_\eta\rangle$. The proof of the equality (64) can be found in Ref. [12].

From the definition of C_η we have,

$$\langle C_\eta\rangle = p\times 1 + (1-p)\times 0 \tag{67}$$

$$= p, \tag{68}$$

$$\langle C_\eta^2\rangle = p\times 1^2 + (1-p)\times 0^2 \tag{69}$$

$$= p, \tag{70}$$

where p is the probability of occurrence of the value η over the ensemble, that is, if the system is ergodic, $p = \overline{\rho(\eta)}\Delta\eta$. Then,

$$\langle C_\eta^2\rangle - \langle C_\eta\rangle^2 = \overline{\rho(\eta)}\Delta\eta\left(1-\overline{\rho(\eta)}\,\Delta\eta\right) \simeq \overline{\rho(\eta)}\,\Delta\eta. \tag{71}$$

Inserting Eq. (71) in Eq. (64) yields the required result.

Appendix C. Code for the iteration loop

This is the code, based on Eq. (15), used to compute the free energies f_i. Different optimizations have been included that greatly reduce the computational time. The free energies are shifted (in respect to f_0) and inserted in the RHS of Eq. (15) as soon as they are available. This procedure reduces the number of iterations necessary to achieve convergence. The Boltzmann factors $\exp[-\beta W_k(\mathbf{R}_{i,l})]$ are precomputed and stored in a three-dimensional array, and the factors $n_k \times \exp[\beta f_k]$ are computed outside of the most inner loop. These last two optimizations greatly reduce the CPU time per iteration.

`Nwind`:	number of windows
`Niter`:	maximum number of iterations
`nt[i]`:	n_i
`ebf[k]`:	$\mathrm{e}^{+\beta f_k}$
`ebf2[k]`:	buffer for $\mathrm{e}^{-\beta f_k}$
`ebw[i][l][k]`:	$\mathrm{e}^{-\beta W_k(\mathbf{R}_{i,l})}$
`fact[k]`:	$n_k \times \mathrm{e}^{+\beta f_k}$

```
for(k=1;k<=Nwind;k=k+1)                    #
{                                          #
   fact[k]=nt[k]*ebf[k] ;                  # initialize the array fact
}                                          #
                                           #
```

```
for(n=1;n<=Niter;n=n+1)                          # start the iteration
{                                                #
  for(k=1;k<=Nwind;k=k+1)                        # loop over windows
  {                                              #
    ebfk=zero;                                   #
    for(i=1;i<=Nwind;i=i+1)                      # loop over windows
    {                                            #
      for(l=1;l<=nt[i];l=l+1)                    # loop over times series
      {                                          #
        bottom=zero;                             #
        for(j=1;j<=Nwind;j=j+1)                  # most inner loop
        {                                        #
          bottom=bottom+ebw[i][l][j]*fact[j];# compute the denominator
        }                                        #
        ebfk=ebfk+ebw[i][l][k]/bottom;           # sum the integrand
      }                                          #
    }                                            #
    ebf2[k]=ebfk;                                # save in buffer
    ebf[k]=1/(ebf[1]*ebfk);                      # shift the new free energy
    fact[k]=nt[k]*ebf[k];                        # replacement
  }                                              #
                                                 #
  conv=1;                                        # convergence flag
  for(k=1;k<=Nwind;k=k+1)                        #
  {                                              #
    delta=ABS(kbt*log(ebf[k]/ebf2[k]));          # compare new and old free
                                                 #   energies
    if(delta>=tol) conv=0;                       # test the convergence
    ebf[k]=ebf2[1]/ebf2[k];                      # shift the free energies
  }                                              #
  if(conv>0) break;                              # if convergence, exit the loop
}                                                # end of the iteration loop
```

References

[1] P. Kollman, Chem. Rev. 93 (1993) 2395.
[2] W.F. van Gunsteren, P.K. Weiner (Eds.), Computer Simulation of Biomolecular Systems, ESCOM, Leiden, 1989.
[3] J.G. Kirkwood, J. Chem. Phys. 3 (1935) 300.
[4] A.M. Ferrenberg, Phys. Rev. Lett. 63 (1989) 1195.
[5] S. Kumar, D. Bouzida, R.H. Swendsen, P.A. Kollman, J.M. Rosenberg, J. Comput. Chem. 13 (1992) 1011.
[6] C.M. Bennet, J. Comput. Chem. 22 (1976) 245–268.
[7] B. Roux, Comput. Phys. Commun. 91 (1995) 275.
[8] M. Nina, D. Beglov, B. Roux, J. Phys. Chem. B 101 (1997) 5239.
[9] D.A. Pearlman, J. Phys. Chem. 98 (1994) 1487.
[10] C. Chipot, P.A. Kollman, D.A. Pearlman, J. Comput. Chem. 17 (1996) 1112.
[11] G.M. Torrier, J.P. Valleau, Chem. Phys. Lett. 28 (1974) 578.
[12] H. Müller-Krumbhaar, K. Binder, J. Stat. Phys. 8 (1973) 1.
[13] X. Kong, C.L. Brooks, J. Phys. Chem. 105 (1996) 2414.

[14] C. Bartels, M. Karplus, J. Comput. Chem. 18 (1997) 1450.
[15] C. Bartels, M. Karplus, J. Phys. Chem. 102 (1998) 865.
[16] E.M. Boczko, C.L. Brooks, J. Phys. Chem. 97 (1993) 4509.
[17] F.B. Scheinerman, C.L. Brooks, J. Mol. Biol. 278 (1998) 439.
[18] S.O. Samuelson, G.J. Martyna, J. Chem. Phys. 109 (1998) 11061.
[19] B.R. Brooks, R.E. Bruccoleri, B.D. Olafson, D.J. States, S. Swaminathan, M. Karplus, J. Comput. Chem. 4 (1983) 187.
[20] D. Beglov, B. Roux, J. Chem. Phys. 100 (1994) 9050.
[21] W.L. Jorgensen, J. Chandrasekhar, J.D. Madura, R.W. Impey, M.L. Klein, J. Chem. Phys. 79 (1983) 926.
[22] R.W. Zwanzig, J. Chem. Phys. 22 (1954) 1420–1426.